ISBN: 978-3-95450-208-0 doi:10.18429/JACoW-IPAC2019-MOPGW047

ANALYSIS AND SIMULATION OF THE "AFTER-PULSE" RF BREAKDOWN

Xiancai Lin [1,2], Hao Zha[1,2], Jiaru Shi[1,2*], Huaibi Chen[1,2], Xiaowei Wu[3], Zening Liu[1,2]
[1] Department of Engineering Physics, Tsinghua University, Beijing 100084, PR China
[2] Key Laboratory of Particle and Radiation Imaging of Ministry of Education, Tsinghua University, Beijing 100084, PR China
[3] CERN, Geneva, Switzerland

Abstract

During the high power experiment of a single-cell standing-wave accelerating structure, it was observed that many RF breakdowns happen when the field inside cavity is decaying after the input rf pulse is off. The distribution of breakdown timing shows a peak at the moment of RF power switches off. A series of simulation was performed to study the after-pulse breakdown effect in such a standing-wave structure. A method of calculating poynting vector over time is proposed in this article to study the modified poynting vector at critical points in the cavity. Field simulation and thermal calculation were also carried out to analyse possible reasons for the after-pulse breakdown effect.

INTRODUCTION

RF breakdown is one of the main limitation to achieve high gradient accelerating structures [1], however, its mechanism still haven't been fully understood over decades of research. During this period, several physical parameters that affect breakdown rate (BDR) have been studied and proposed as a guidance for the design and optimization of high gradient structures, such as frequency, electric field, pulse heating, rf power and modified Poynting vector [2] .

Recent years, a series of accelerator structures fabricated at Tsinghua University were high-gradient tested at the New X-band Test Facility (Nextef) in High Energy Accelerator Research Organization(KEK). The breakdown timing inside a pulse (which is the time delay between the beginning of the rf pulse and the breakdown, as shown in Fig. 1 (a)) of these structures is analysed. Among these results, it was observed in one of the structures, THU-REF[1], with different pulse duration time, that the breakdown timing distribution has a peak after the input rf power is off, which is called after-pulse breakdown effect, as shown in Fig. 1 (b)-(d). Basic parameters of the test environment are listed in Table 1 [1].

The BDR is supposed to have a positive correlation with the electric field, which contradicts with this phenomenon. Possible reasons to explain this include:

- After RF power switches off, the abrupt change of input power gives rise to higher order mode, which causes the breakdown.
- There is a large power flow out of the cavity when RF power is off, which makes the modified Poynting vector turn large.
- The accumulation of heat produced by RF pulse lead to the breakdown.

A series of simulation was performed based on these assumption to study the after-pulse breakdown effect, as will be illustrated in the next chapter.

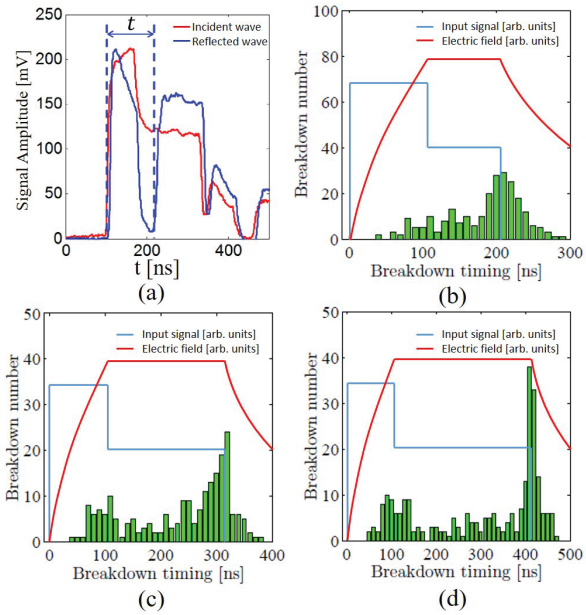

Figure 1: Detected signal and breakdown timing distribution. (a) Typical breakdown signal. t is the breakdown timing. (b-d) Breakdown timing distribution in THU-REF with 200 ns, 300 ns and 400 ns pulse width.

Table 1: Test Environment of REF in Nextef

Parameter	Value
Frequency	11.424 GHz
Peak Power	15 MW
Pulse Duration	200/300/400 ns
Total Pulse Number	1.21×10^8
Breakdown Event Number	1267

* shij@tsinghua.edu.cn
[1] THU-REF is a standing-wave structure built in Tsinghua University served as a reference cavity for choke mode accelerating structures

ISBN: 978-3-95450-208-0 doi:10.18429/JACoW-IPAC2019-MOPGW047

SIMULATION

To study the time response of the standing-wave structure stimulated by a time-varying signal(pulse), simulation was performed with time domain solver in CST [3]. The 3D model and input signal are shown in Fig. 2.

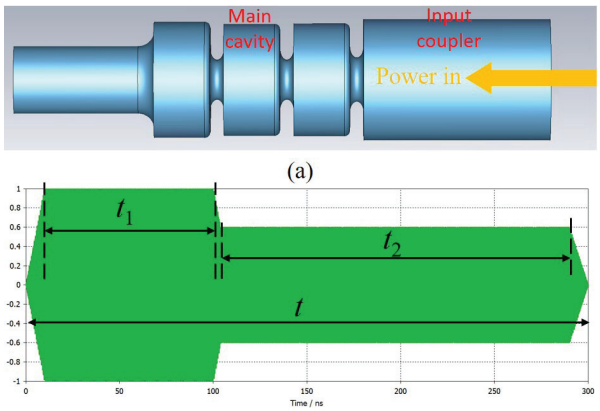

Figure 2: THU-REF 3D model in CST and its input signal. (a) THU-REF 3D model. Power is input from the wave guide port at the right side, which represents power from the input coupler. (b) Input signal for the wave guide port. The signal is stair-like to make a flat top in the field. t_2 could be modified to change the signal time t(pulse width).

Field Simulation

To monitor the field versus time, several probes were placed inside the model. One of the probes was set on the centre of the main cavity to observe the accelerating field, as shown in Fig. 3 (a). The amplitude and Fourier transform of the accelerating electric field was also shown. The amplitude of the electric field shows good consistence with the theory. The discrete Fourier transform of the field between 280 and 300 ns illustrates that there's no obvious other modes in the cavity. Field at other points have similar patterns. The result shows that no HOMs were stimulated when the power is off.

Transient Complex Poynting Vector Calculation

A. Grudiev et. al. proposed modified Poynting vector as a new gradient limiting factor [4]:

$$S_c = \mathrm{Re}\{\bar{S}\} + g_c \cdot \mathrm{Im}\{\bar{S}\} \tag{1}$$

$\bar{S}$ is the Complex Poynting vector in frequency domain. Its real part, $\mathrm{Re}\{\bar{S}\}$, describes the active power flow and its imaginary part, $\mathrm{Im}\{\bar{S}\}$, describes the reactive power flow. g_c is the weighting factor [4].

To analyse the breakdown timing distribution, an idea is to calculate the complex Poynting vector over time. Assume that the input signal in Fig.2 (b) can be expressed as the complex form $A(t)e^{j\omega t}$. Therefore, the field at a point inside the model should have a similar expression $E(t)e^{j(\omega t+\varphi_1)}$ and

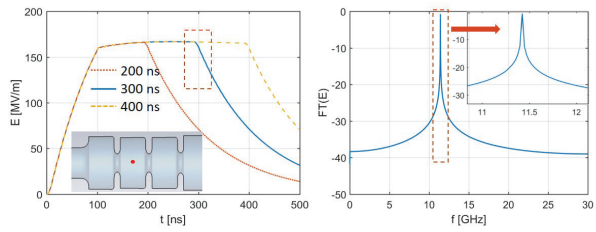

Figure 3: Electric field amplitude and its Fourier transform. (a) Electric field amplitude at the centre of the main cavity(the red point) of different pulse duration. The field between 280 and 300 ns(the red dotted rectangle) was taken to perform discrete Fourier transform. (b) Fourier transform of the electric field between 280 and 300 ns. It shows that no adjacent modes or HOMs were stimulate when the power is off.

$H(t)e^{j(\omega t+\varphi_2)}$. Nevertheless, the field measured or simulated in time domain is its real part. Here's the way to calculate its imaginary part from the real one.

Take electric field as an example. Suppose its real part's form is $\mathrm{Re}\{\bar{E}(t)\} = E(t)\cos(\omega t)$, where the phase term are neglected. A time step Δt later, the field will be $E(t+\Delta t)\cos[\omega(t+\Delta t)]$. Since Δt is much smaller than the field amplitude varying time, $E(t) \approx E(t+\Delta t)$. According to:

$$\cos[\omega(t+\Delta t)] = \cos(\omega t)\cos(\omega\Delta t) - \sin(\omega t)\sin(\omega\Delta t) \tag{2}$$

the imaginary part of electric field can be calculated as:

$$\begin{aligned}\mathrm{Im}\{\bar{E}(t)\} &= E(t)\sin(\omega t) \\ &= \frac{\mathrm{Re}\{\bar{E}(t)\}\cos(\omega\Delta t) - \mathrm{Re}\{\bar{E}(t+\Delta t)\}}{\sin(\omega\Delta t)}\end{aligned} \tag{3}$$

The imaginary part of Magnetic field can be obtained in the same way. After the complex field was accomplished, the complex Poynting vector could be calculated by:

$$\bar{S}(t) = \frac{1}{2}\,\bar{E}^*(t) \times \bar{H}(t) \tag{4}$$

Nine probes were placed near the iris(as shown in Fig. 4 (a)), and the field of them were exported to derive the transient complex Poynting vector. Only results of probes 4-8 in the main cavity are shown(Fig. 4 (b)-(g)) because field is higher here. $\mathrm{Re}\{\bar{S}\}$ calculated at point 3 to 9 have strong oscillation part. Its Fourier transform shows two peaks at 0.09 GHz and 0.14 GHz, which shows accelerating mode(11.424 GHz) couples with $\pi/2$ mode(11.33 GHz) and 0 mode(11.28 GHz). This oscillation part was weaken by eliminating unwanted peaks in frequency domain.

Real part of Poynting vector shows the net power flow. Positive value means there's net power flow into the structure and vice versus. Imaginary part of Poynting vector represents the field strength. Plus sign means the field is inductive, or electric field lags behind magnetic field. Probes 5, 6 have

ISBN: 978-3-95450-208-0 doi:10.18429/JACoW-IPAC2019-MOPGW047

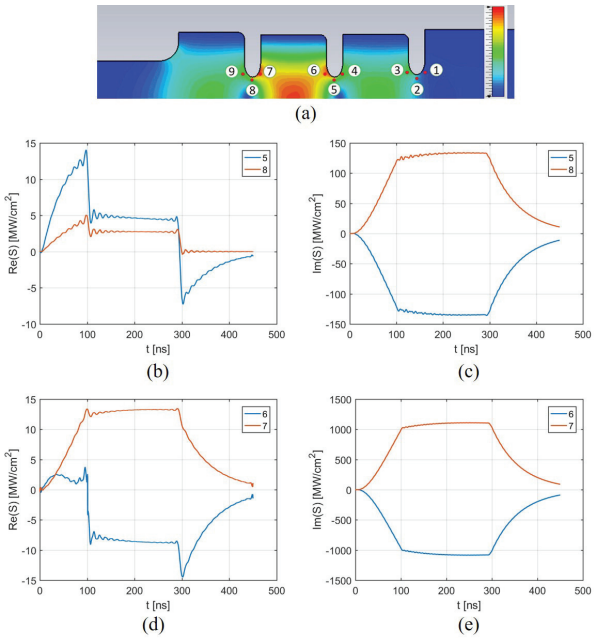

Figure 4: Transient complex Poynting vector at the iris. (a) Eigen field amplitude of the structure and positions of probes. (b)(d) Real part of $\bar{S}$ of probes 5,8 and 6,7. (c)(e) Imaginary part of $\bar{S}$ of probes 5,8 and 6,7.

a relatively high power flow out of the structure at the moment when the power is off. According to equation (1), when adding the real part and the imaginary part, it would make a peak value at when the rf power is off, as shown in Fig. 5. However, the imaginary part is much bigger than real part in probe 6, the peak is not evident.

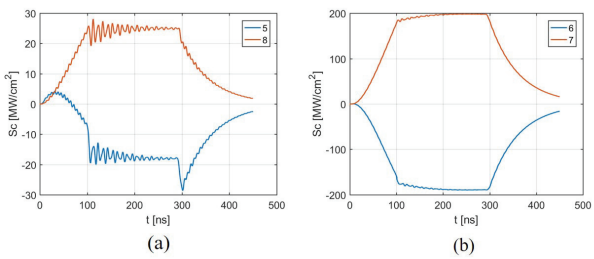

Figure 5: Modified Poynting vector at probes. Weighting factor g_c is 1/6. (a) Modified Poynting vector at probe 5, 8. (b) Modified Pynting vector at probe 6,7.

Pulse Heating Calculation

For short pulses, thermal conduction of every point on the surface of the cavity could be regarded as on a one-dimensional semi-infinite slab. Based on this, the temperature rise by pulse heating derived in [5] is:

$$\Delta T(t) = \frac{1}{\sqrt{\pi \rho c_\varepsilon k}} \int_0^t \frac{R_s |H_\parallel(t')|^2}{2\sqrt{t-t'}} \mathrm{d}t' \qquad (5)$$

In the formula, ρ is the density of cavity material, c_ε is its specific heat capacity, and k is coefficient of heat conduction. These parameter are listed in Table 2 [5].

Table 2: Parameters of Fully Annealed OFE Copper at Room Temperature

Parameter	Value
ρ	8.95×10^3 kg/m^3
c_ε	385 J/kg · K
k	391 W/m · K

The peak surface magnetic field point lays at the middle of the main cavity's side wall, as shown in Fig. 6. The results shows the temperature rise reaches its maximum at the end of the pulse. ΔT is 12 K, 15 K, 18 K for 200 ns, 300 ns, 400 ns pulse respectively at a power level of 15MW.

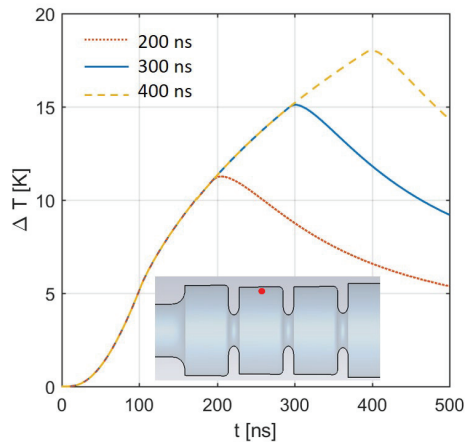

Figure 6: Temperature rise at the peak surface magnetic field point at a power level of 15MW. The results shows the temperature rise reaches its maximum at the end of the pulse.

CONCLUSION

Results of field simulation, complex Poynting vector and pulse heating calculation are analyzed in this paper. It reveals that modified Poynting vector in time domain and temperature rise within the pulse are possible reasons account for the after pulse breakdown effect. A simple method to calculate the imaginary part in a time-harmonic like field was proposed, it works well when field variation is much slower than the filed oscillation.

REFERENCES

[1] Xiaowei Wu, "Design and Experiment of X-band High-gradient Choke-mode AcceleratingStructure", Ph. D Thesis, Tsinghua University, 2017.

[2] Jiahang Shao, "Investigations on rf Breakdown Phenomenon in High Gradient Accelerating Structures", Ph. D Thesis, Tsinghua University, 2017.

ISBN: 978-3-95450-208-0 doi:10.18429/JACoW-IPAC2019-MOPGW047

[3] CST, https://www.cst.com

[4] A. Grudiev, S. Calatroni, and W. Wuensch, "New local field quantity describing the high gradient limit of accelerating structures", in *Physical Review Special Topics-Accelerators and Beams*, 12.10 (2009): 102001.

[5] D.Pritzkau, “RF Pulsed Heating”, Ph. D Thesis, SLAC-R-577, 2001.